submitted to
PHYSICAL REVIEW B VOLUME XXX NUMBER XXX MONTH XXX

Curie temperature of anisotropic ferromagnetic films

D. A. Garanin*
Max-Planck-Institut für Physik komplexer Systeme, Nöthnitzer Strasse 38, D-01187 Dresden, Germany

(Received 16 June 1998)

Dimensional crossover of ordering in ferromagnetic films with both periodic and free boundary conditions is studied for the exactly solvable uniaxial model of classical D-component spin vectors in the limit $D \to \infty$. Analytical and numerical solution of the exact equations describing this model shows that for lattice dimensionalities $d > 4$, finite-size corrections to the bulk values of T_c are characterized by the mean-field exponents and anisotropy-dependent amplitudes. For $d \leq 4$, the mean-field behavior is only realized in the region $\kappa_c N \gg 1$, where κ_c is the dimensionlesss inverse *transverse* (with respect to the easy axis) bulk correlation length at T_c and N is the number of layers in the film. In the region $\kappa_c N \ll 1$ and the dimensionality range $3 < d \leq 4$, finite-size corrections are described by the universality class of the isotropic $D = \infty$ model. For $d \leq 3$, magnetic ordering vanishes in the isotropic limit, $\kappa_c \to 0$, since the film behaves as an object of dimensionality $d' = d - 1 \leq 2$ and long-wavelength fluctuations destroy the order. Here the suppression of T_c of a film can be substantial, depending on the competition between the weakening anisotropy and the increasing film thickness. For thick films, T_c becomes small only for very small anisotropy.

PACS number(s): 64.60.Cn, 75.10.Hk, 75.30.Pd, 75.70.Ak

I. INTRODUCTION

Ferromagnetic ordering in the film geometry shows a dimensional crossover on the film thickness, which is measured by the number of layers N for the lattice spacing a_0 set to unity, and on the closeness to the Curie point T_c. For a spatial dimensionality d, thick films, $N \gg 1$, show a d-dimensional behavior far enough from T_c. On the other hand, in the close vicinity of T_c the film behaves as an object characterized by the reduced dimensionality $d' = d - 1$. The latter regime is realized for $\xi_c \gtrsim N$, where ξ_c is the dimensionless bulk correlation length. An important implication of this dimensional crossover is that isotropic Hamiltonians cannot describe ordering of films in three dimensions. Indeed, since films behave two dimensionally at the would be critical point, the long-wavelength fluctuations (spin waves, Goldstone modes) preclude ordering. Due to the exponential increase of the correlation length with lowering temperature, two-dimensional magnets are extremely sensitive to the uniaxial anisotropy which stabilizes order. It is intuitively clear that the stabilizing effect of the anisotropy in thick films should be much stronger than that in usual two-dimensional systems.

Finite-size effects and crossovers between different universality classes in thin magnetic films have been observed in a number of experiments.[1,2,3,4,5,6] The suppression of T_c and other effects in films of arbitrary thickness N are frequently addressed with the spatially-inhomogeneous mean-field approach of Ref. 7, which, naturally, misses the influence of Goldstone modes on ordering mentioned above. The general large-N asymptotic form of the T_c-shift in thick films is given by

$$[T_c(\infty) - T_c(N)]/T_c(\infty) \cong A/N^{\lambda}, \tag{1.1}$$

as was initially established by the high-temperature series expansions (HTSE) for the Ising model.[8,9] For the exponent λ the finite-size scaling theory[10,11] yields $\lambda = 1/\nu_b$, where ν_b is critical index for the bulk correlation length. The coefficient A in Eq. (1.1) should depend on the anisotropy. For spatial dimensions $d \leq 3$, it should strongly increase with approaching the isotropic limit, so that for any thickness N the right-hand side (rhs) of Eq. (1.1) eventually approaches the value of 1. In this case of a substantial suppression of T_c, the functional form of Eq. (1.1) is no longer valid. For very small uniaxial anisotropy, the film orders at such low temperatures that all spins along the direction perpendicular to the surface are strongly correlated and can be considered as a single composite spin. Thus the film is mapped on d'-dimensional monolayer with the exchange interaction NJ. For the model with a uniaxially anisotropic exchange, the anisotropy of the exchange interaction $\eta' \ll 1$ is replaced by $d\eta'/(d-1)$, since the composite spins acquire an "internal" anisotropy. In this case one has

$$T_c[d, J, \eta', N] \cong T_c[d-1, NJ, d\eta'/(d-1), 1]. \tag{1.2}$$

For the model with a single-site anisotropy, the latter, relative to the exchange, is not renormalized. It seems that no one of conventional theories can reproduce the crossover between the two regimes described by Eqs. (1.1) and (1.2).

The effects of would be Goldstone modes on ordering in weakly-anisotropic low-dimensional magnetic structures

can be conveniently studied within the exactly solvable anisotropic spherical model (ASM) which is the limit $D \to \infty$ of the classical D-component spin-vector model. The Hamiltonian of the latter has the form

$$\mathcal{H} = -\frac{1}{2}\sum_{ij} J_{ij}\left(m_{zi}m_{zj} + \eta\sum_{\alpha=2}^{D} m_{\alpha i}m_{\alpha j}\right), \qquad (1.3)$$

where $\mathbf{m}_i$ is the normalized D-component vector, $|\mathbf{m}_i| = 1$, and $\eta \equiv 1 - \eta' \leq 1$ is the dimensionless anisotropy factor. In the isotropic case, $\eta = 1$, the partition function of this model coincides in the limit $D \to \infty$ (Ref. 12) with that of the spherical model (SM).[13] There are, however, a number of essential differences between both models. In particular, the spherical model yields unphysical negative coefficient A in Eq. (1.1) for the film with free boundary conditions (fbc) because of the global spin constraint.[14] Improved versions of the SM without the global spin constraint[15,16] yield positive A, as it should. However, within the SM the problem can be only considered in four dimensions, since the SM cannot be done anisotropic and in three dimensions T_c is zero for all finite values of N.

By contrast, the ASM describes ordering of bulk samples in low dimensions,[17] since anisotropy gives rise to the gap for spin fluctuations. In Ref. 18 it was shown that even in the isotropic case there are different, longitudinal and transverse correlation functions (CF) in the ASM below T_c, in contrast to the inherently single CF in the SM. The ASM correlation functions have a kind of spin-wave form, which is, however, valid in the whole range of temperatures. This makes the ASM a convenient tool for the investigation of classical spin systems at elevated temperatures at the level beyond the mean-field approximation (MFA). Whereas the critical coupling of fluctuations dies out in the limit $D \to \infty$ and the critical behavior is simplified, the not less important *qualitative* effects of the would be Goldstone modes on ordering are accounted for in the "pure" form. The most recent example of the application of the ASM to the spatially-homogeneous systems is Ref. 19, where the spin-liquid state of the classical antiferromagnet on the kagomé lattice is considered.

In the inhomogeneous case, the closed lattice-based system of equations describing the ASM was obtained in Ref. 20. This system of equations has been analytically solved in the domain-wall geometry for the *biaxial* generalization of the Hamiltonian (1.3). This model features a phase transition of an interface, which can be described analytically beyond the MFA and observed in experiment.[21] A more complicated situation is realized in the semi-infinite geometry, where analytical solutions can be only obtained in particular and limiting cases and application of numerical methods is necessary. In Ref. 22 the correlation functions of the semi-infinite ferromagnet have been computed at $T \geq T_c$ in the case of the so-called ordinary phase transition (the transition at the surface, that is characterized by its own set of critical indices, is driven by the phase transition in the bulk). For the film geometry, the problem becomes even more difficult because of the additional effect — suppression of T_c in comparison to its bulk value. In my preceding Letter on ferromagnetic films, Ref. 23, only some analytical results for $N \gg 1$ have been obtained, but no numerical calculations have been performed.

The aim of this paper is a complete solution for the correlation functions and Curie temperatures of ferromagnetic films within the ASM in the whole range of parameters with the use of the numerical algorithm of Ref. 22. In contrast to Ref. 23, calculations will be performed for the model with a continuous spatial dimensionality d, which has been introduced in Ref. 22. The latter is interesting, in particular, since in the isotropic limit nontrivial finite-size corrections to T_c, which differ from the mean-field ones, are only realized in the dimensionality range between three and four. In addition, analytical resultes will be given for ferromagnetic films consisting of a few layers.

The main part of this paper is organized as follows. In Sec. II the basic equations describing the anisotropic spherical model and the methods of their solution are be briefly reviewed. In Sec. III the analytical solutions for the simplified model with periodic boundary conditions (pbc) are given. In Sec. IV the available analytical solutions for the film with free boundary conditions are considered. In Sec. V the corresponding numerical results are presented. In Sec. VI the results obtained and some possible extensions of the model are discussed.

II. BASIC RELATIONS

At or above T_c in zero field, the magnetization $\mathbf{m}_i$ is zero and the ASM is described by the closed system of equations for the correlation functions of transverse ($\alpha \geq 2$) spin components, $s_{ij} \equiv D\langle m_{\alpha i}m_{\alpha j}\rangle$, and the spatially varying gap parameter, G_i. More general forms of these equations with $\mathbf{m}_i \neq 0$ and a lot of other details can be found in Refs. 20, 23 and 22; here only the most important formulas will be given. In the geometry considered, it is convenient to use the Fourier representation in $d' = d - 1$ translationally invariant dimensions parallel to the surface and the site representation in the dth dimension. For the model with nearest-neighbor (nn) interactions, the equation for the Fourier-transformed CF $\sigma_{nn'}(\mathbf{q})$ then takes the form of a system of the second-order finite-difference equations in the set of layers $n = 1, 2, ..., \infty$,

$$2b_n\sigma_{nn'} - \sigma_{n+1,n'} - \sigma_{n-1,n'} = (2d\theta/\eta)\delta_{nn'}, \qquad (2.1)$$

where b_n is given by

$$b_n = 1 + d[(\eta G_n)^{-1} - 1] + d'(1 - \lambda'_{\mathbf{q}}) \qquad (2.2)$$

and $\lambda'_{\mathbf{q}}$ for the d-dimensional hypercubic lattice reads

$$\lambda'_{\mathbf{q}} = \frac{1}{d'}\sum_{i=1}^{d'} \cos(q_i). \qquad (2.3)$$

In Eq. (2.1), θ is the reduced temperature defined by

$$\theta \equiv \frac{T}{T_c^{\rm MFA}(\infty)}, \qquad T_c^{\rm MFA}(\infty) = \frac{2dJ}{D} \tag{2.4}$$

The quantities $\sigma_{0,n'}$ and $\sigma_{N+1,n'}$ in the nonexisting layers, which enter equations (2.1) at the film boundaries $n = 1$ and $n = N$, are set to

$$\begin{array}{ll} \sigma_{0,n'} = \sigma_{N+1,n'} = 0, & \text{(fbc)} \\ \sigma_{0,n'} = \sigma_{N,n'}, \qquad \sigma_{N+1,n'} = \sigma_{1,n'}, & \text{(pbc)} \end{array} \tag{2.5}$$

as the free and periodic boundary conditions. The autocorrelation functions in each of the N layers, s_{nn}, satisfy the set of constraint equations

$$s_{nn} \equiv \int \frac{d^{d'}\mathbf{q}}{(2\pi)^{d'}} \sigma_{nn}(\mathbf{q}) = 1, \tag{2.6}$$

which are the consequence of the spin rigidity, $|\mathbf{m}_i| = 1$. A straightforward algorithm for the numerical solving the equations above is, for a given set of G_n, to compute all σ_{nn} from the system of linear equations (2.1) and then to put the results in Eq. (2.6) to obtain, after the integration over the Brillouin zone, the set of nonlinear equations for G_n. After G_n have been found, one can compute the longitudinal CF $\sigma^{zz}_{nn'}$ from Eqs. (2.1) and (2.2), where η is set to 1.

For thick films far from the boundaries, it is convenient to consider the deviation form the bulk value

$$G_{1n} \equiv G_n - G \ll 1, \tag{2.7}$$

that is proportional [and for $T \le T_c(\infty)$ equal] to the inhomogeneous part of the reduced energy pro site $\tilde{U}_{1n}$ (see Ref. 22). The bulk gap parameter G satisfies the equation

$$\theta G P(\eta G) = 1, \tag{2.8}$$

where

$$P(X) \equiv \int \frac{d^d\mathbf{k}}{(2\pi)^d} \frac{1}{1 - X\lambda_{\mathbf{k}}} \tag{2.9}$$

is the lattice Green function. The quantity $\lambda_{\mathbf{k}} \equiv J_{\mathbf{k}}/(2dJ)$ for the nn interaction is given by Eq. (2.3) with $d' \Rightarrow d$ and $\mathbf{q} \Rightarrow \mathbf{k}$. The solution G of Eq. (2.8) increases with lowering temperature θ; at $G = 1$ the gap in the longitudinal CF closes, longitudinal susceptibility diverges, and the phase transition occurs. This defines the bulk transition temperature[17]

$$\theta_c(\infty) = 1/P(\eta), \tag{2.10}$$

that generalizes the well known result for the spherical model $\theta_c = 1/P(1)$ (Ref. 13). The lattice Green function $P(X)$ satisfies $P(0) = 1$ and has a singularity at $X \to 1$, the form of which in different dimensions can be found in Ref. 22. For $d \le 2$, the Watson integral $W \equiv P(1)$ goes to infinity; thus formula (2.10) yields nonzero values of the Curie temperature only for the anisotropic model, $\eta < 1$. It should be noted that in the anisotropic case the critical indices of the model coincide with the mean-field ones due to the suppression of the singularity of $P(\eta G)$ for $G \to 1$. Below θ_c, the spontaneous magnetization appears, and G sticks to 1.

For $n \gg 1$, $q \ll 1$, and $\kappa \ll 1$, where κ is the inverse transverse correlation length defined by

$$\kappa^2 \equiv 2d[1/(\eta G) - 1] \cong 2d[1 - \eta G] \ll 1, \tag{2.11}$$

one can reduce the second-order finite-difference equation (2.1) to the differential equation for the Green's function

$$\left(\frac{d^2}{dn^2} - \tilde{q}^2 + 2dG_{1n}\right)\sigma_{nn'} = -2d\theta\delta(n - n'), \tag{2.12}$$

where n is considered as a continuous variable, $\tilde{q} \equiv \sqrt{\kappa^2 + q^2}$, and G_{1n} is defined by Eq. (2.7). Note that the transverse bulk correlation length $\xi_{c\perp} \equiv \xi_{c\alpha} \equiv 1/\kappa$ increases without diverging with decreasing temperature down to θ_c and remains constant below θ_c, in accordance with the behavior of G. The critical-point value

$$\kappa_c^2 \equiv 2d[1/\eta - 1] \tag{2.13}$$

measures the anisotropy and varies between 0 for the isotropic model and ∞ for the classical Ising model. Analytical solution of Eq. (2.12) is only possible in particular cases, when G_{1n} has a simple form and can be guessed. In the domain-wall geometry, $G_{1n} \propto 1/\cosh^2[(n-n_0)/\delta]$, where n_0 corresponds to the center of the domain wall and δ is the self-consistently determined domain-wall width.[20] Accordingly, the solution for $\sigma_{nn'}$ is a combination of hyperbolic and exponential functions. For the isotropic semi-infinite ferromagnet at the ordinary phase transition in the dimensionality range $2 < d < 4$ the form of G_{1n} is[24,22]

$$G_{1n} = \frac{\frac{1}{4} - \mu^2}{2dn^2}, \qquad \mu = \frac{d-3}{2}, \tag{2.14}$$

and $\sigma_{nn'}$ can be expressed through the modified Bessel functions $I_\mu(qn)$ and $K_\mu(qn)$.

Note that long-wavelength equation (2.12) is valid for continuous lattice dimensionalities d and its solution in the asymptotic region $n \gg 1$ is universal. The disadvantage of Eq. (2.12), however, is that it cannot be solved numerically in confined geometries, which is desirable in most cases (e.g., for a semi-infinite ferromagnet away from criticality) when there is no analytical solution. The problem is the strong divergence of G_{1n} near the boundaries [see Eq. (2.14)] and the ensuing loss of the boundary condition. In fact, however, this divergence is an artifact of the continuous approximation. The lattice-based calculation of Ref. 22 for the simple cubic lattice at isotropic criticality yields, on the contrary, rather small values of G_{1n} near the boundary: $G_{11} = 0.09615$, $G_{12} = 0.01254$, $G_{13} = 0.00532$, $G_{14} = 0.00291$, etc. To get access to continuous dimensionalities while perserving the discrete structure of the lattice in the direction perpendicular to

the surface, a special kind of a "lattice" has been introduced in Ref. 22. This lattice is characterized by the Fourier-transformed exchange interaction $J_{\mathbf{k}} \equiv J_0 \lambda_{\mathbf{k}}$ of the form

$$\lambda_{\mathbf{k}} \equiv \frac{1}{d}\cos k_z + \frac{d'}{d}\lambda'_{\mathbf{q}}, \qquad \lambda'_{\mathbf{q}} \Rightarrow 1 - \frac{q^2}{2d'} \tag{2.15}$$

[cf. Eq. (2.3)] with a continuous $d' = d - 1$ and *in the whole Brillouin zone*. The natural hypercubic cutoff $|k_i| \le \pi$ and the corresponding density of states are modified for the $\mathbf{q}$ components according to

$$\int \frac{d^{d'}\mathbf{q}}{(2\pi)^{d'}} \ldots \Rightarrow \frac{d'}{\Lambda^{d'}} \int_0^{\Lambda} dq q^{d'-1} \ldots \tag{2.16}$$

with $\Lambda = \sqrt{2(d+1)}$. This choice of Λ preserves the usual sum rules for the exchange interaction. Numerical calculations of Ref. 22 on the continuous-dimension lattice confirmed formula (2.14) in the asymptotic region, $n \gg 1$. Near the boundary, deviations from universality have been detected. In particular, for the continuous dimensionality $d = 3.0$ one obtains $G_{11} = 0.10672$, $G_{12} = 0.01195$, $G_{13} = 0.00495$, $G_{14} = 0.00270$, etc., which deviates from the results for the simple cubic lattice quoted above.

If the gap parameter G_n is uniform, as in the bulk or in a film with periodic boundary conditions, Eq. (2.1) can be solved analytically in a straightforward way. In other cases, an efficient numerical algorithm is needed. One possibility, which is used in Ref. 22 and in the present article, is to represent the layer-layer autocorrelation function σ_{nn} in the continued-fraction form[23,22]

$$\sigma_{nn} = \frac{2d\theta}{\eta} \frac{1}{2b_n - \alpha_n - \alpha'_n}, \tag{2.17}$$

where b_n is given by Eq. (2.2) and the functions α_n and α'_n are found from the forward and backward recurrence relations

$$\alpha_{n+1} = \frac{1}{2b_n - \alpha_n}, \qquad \alpha'_{n-1} = \frac{1}{2b_n - \alpha'_n} \tag{2.18}$$

with boundary conditions $\alpha_1 = \alpha'_N = 0$. The nondiagonal CFs can then be written as

$$\sigma_{nn'} = \sigma_{nn} \times \begin{cases} \prod_{l=n}^{n'-1} \alpha'_l, & n' > n \\ \prod_{l=n}^{n'+1} \alpha_l, & n' < n. \end{cases} \tag{2.19}$$

In the bulk the quantity b of Eq. (2.2) is independent of n, and Eqs. (2.18) can be solved to give

$$\alpha = b - \sqrt{b^2 - 1} = \alpha', \tag{2.20}$$

The solution the spin CFs above thus simplifies to the result

$$\sigma^{\text{bulk}}_{nn'}(\mathbf{q}) = \frac{d\theta}{\eta} \frac{\alpha^{|n-n'|}}{\sqrt{b^2-1}}, \tag{2.21}$$

that can also be obtained with other methods. For the numerical solution in the film geometry, diagonal CFs σ_{nn} of Eqs. (2.17) should be substituted into the contraint equations (2.6), which defines the variation of G_n after application of some iterative scheme (e.g., Newton method).

There is another routine for solving system of equations (2.1) and (2.6), which avoids numerical calculation of the integrals over the Brillouin zone at each step.[25] The solution Eq. (2.1) for diagonal CFs σ_{nn} can be written in the form

$$\sigma_{nn} = \frac{2d\theta}{\eta} A^{-1}_{nn}, \tag{2.22}$$

where $\hat{A}^{-1}$ is the inverse of the tridiagonal matrix $\hat{A}$ of Eq. (2.1): $A_{nn} = 2b_n$ and $A_{n,n\pm1} = -1$. It is convenient to represent matrix $\hat{A}$ in the form

$$\hat{A} = \hat{B} - 2d'\lambda'_{\mathbf{q}}\hat{I}, \tag{2.23}$$

where $\hat{I}$ is a unit matrix and $\hat{B}$ is a tridiagonal matrix:

$$B_{nn} = 2d/(\eta G_n), \qquad B_{n,n\pm1} = -1. \tag{2.24}$$

Then Eq. (2.22) can be transformed to

$$\sigma_{nn} = \frac{2d\theta}{\eta} \sum_{\rho=1}^{N} \frac{U^2_{n\rho}}{\lambda_\rho - 2d'\lambda'_{\mathbf{q}}}, \tag{2.25}$$

where $\hat{U}$ is the real unitary matrix ($\hat{U}^{-1} = \hat{U}^T$, i.e., $U^{-1}_{\rho n} = U_{n\rho}$), that diagonalizes $\hat{B}$, and λ_ρ are the eigenvalues of $\hat{B}$. The nice feature of this expression is that $\hat{U}$ and λ_ρ are independent of $\mathbf{q}$. Thus the integral over the Brillouin zone of Eq. (2.25) can be expressed through the lattice Green function of the layers, $P_{d'}$, and constraint equation (2.6) takes the form

$$s_{nn} = \frac{2d\theta}{\eta} \sum_{\rho=1}^{N} \frac{U^2_{n\rho}}{\lambda_\rho} P_{d'}(2d'/\lambda_\rho) = 1. \tag{2.26}$$

Since $P_{d'}(X)$ can be calculated analytically or tabulated, this method should be faster than the continued-fraction formalism described above, especially for hypercubic lattices in high dimensions. However, application of the latter to the semi-infinite ferromagnet in Ref. 22 has shown that it is fast enough, the main problem being the stability of iterations for low dimensionalities d. For this reason, here the continued-fraction formalism is chosen for numerical calculations, whereas the diagonalization method will be applied to find analytical solutions for films consisting of small number of layers.

Before proceeding to the films with free boundary conditions, let us consider the simplified problem with periodic boundary conditions. Here, in an artificial way, all quantities are rendered uniform, but, nevertheless, there is a dimensional crossover discussed above.

III. PERIODIC BOUNDARY CONDITIONS

For the problem with pbc, one has $G_n = G$ and $b_n = b$ in Eq. (2.1). Solving the latter with boundary conditions of Eq. (2.5) yields

$$\sigma_{nn}^{\rm pbc}(\mathbf{q}) = \frac{d\theta}{\eta\sqrt{b^2-1}}\frac{1+\alpha^N}{1-\alpha^N}, \tag{3.1}$$

where $\alpha < 1$ is defined by Eq. (2.20). In the long-wavelength region near criticality, one has

$$\sqrt{b^2-1} \cong \sqrt{\kappa^2+q^2}, \qquad \alpha \cong 1-\sqrt{\kappa^2+q^2}. \tag{3.2}$$

Thus, if $N\sqrt{\kappa^2+q^2} \lesssim 1$, an additional factor $\sqrt{\kappa^2+q^2}$ appears in the denominator of Eq. (3.1), which is responsible for the dimensional crossover in films.

The Curie temperature of a film can be found from the condition that the longitudinal susceptibility diverges. This amounts to vanishing of the determinant of the system of equations for the longitudinal CF at zero wave vector, i.e., Eq. (2.1) with $\eta = 1$ and $\mathbf{q} = 0$. It can be seen that the latter is satisfied for $b(\eta = 1, \mathbf{q} = 0) = 1$ and hence $G = 1$, as in the bulk. Now θ_c can be found from the constraint relation (2.6). Separating the bulk term, one can write

$$\theta_c^{-1} = P_d(\eta) + \frac{d'}{\Lambda^{d'}}\int_0^\Lambda dq q^{d'-1}\frac{2d}{\eta\sqrt{b^2-1}}\frac{\alpha^N}{1-\alpha^N}, \tag{3.3}$$

where, for continuous dimensionalities d, the lattice Green function $P_d(\eta)$ is determined by Eqs. (2.9) and (2.16). For the hypercubic lattice, a usual integration over the Brillouin zone is performed in Eq. (3.3). The large-N asymptotes of Eq. (3.3) can be calculated analytically. For the weakly anisotropic model in the range $d > 3$ and $N\kappa_c \ll 1$, one obtains

$$\theta_c^{-1} \cong P_d(\eta) + \frac{d'}{\Lambda^{d'}}\frac{2d\Gamma(d-2)\zeta(d-2)}{N^{d-2}}. \tag{3.4}$$

For the hypercubic lattice, one should make the replacement

$$d'/\Lambda^{d'} \Rightarrow S_{d'}/(2\pi)^{d'}, \tag{3.5}$$

where $S_d = 2\pi^{d/2}/\Gamma(d/2)$ is the surface of the d-dimensional unit sphere. Dependence of such a type, derived field-theoretically, can be found in Ref. 26. For $3 < d < 4$, it is in accord with finite-size-scaling formula (1.1) with $\lambda = 1/\nu_b = d-2$. In higher dimensions for the $D = \infty$ model one has $1/\nu_b = 2$, whereas the shift exponent λ is given by he same formula. A particular case of Eq. (3.4) is[14,23]

$$\theta_c^{-1} \cong P_4(1) + 2/(3N^2) \tag{3.6}$$

for $d = 4$. For $\kappa_c N \gtrsim 1$, the second term in the rhs of Eq. (3.3), and thus the shift of T_c, decays exponentially with $\kappa_c N$.

In three dimensions, the integral in Eq. (3.3) can be done analytically for all values of $\kappa_c N$, provided $N \gg 1$. For $d = 3$ the result has the form[23]

$$\theta_c^{-1} \cong P_3(\eta) + \frac{3}{\pi N}\ln\frac{1}{1-\exp(-\kappa_c N)}. \tag{3.7}$$

For $\kappa_c N \ll 1$ it simplifies to

$$\theta_c^{-1} \cong P_3(\eta) + \frac{3}{\pi N}\ln\frac{1}{\kappa_c N}. \tag{3.8}$$

For the continuous-dimension lattice $d = 3.0$, the second terrms of the above equations should, according to Eq. (3.5), be multiplied by $\Gamma[(d+1)/2][2\pi/(d+1)]^{(d-1)/2} \Rightarrow \pi/2$. The form of Eq. (3.8) is in accord with finite-size-scaling formula (1.1), but now the coefficient A in Eq. (1.1) depends on anisotropy in a crucial way. In the isotropic limit, κ_c defined by Eq. (2.13) goes to zero, and the logarithmically divergent second term of this formula becomes dominant. In this limit θ_c becomes logarithmically small, in accordance with general formula (1.2), which for the ASM takes the form

$$\theta_c^{-1}(d,\eta,N) \cong \frac{d}{(d-1)N}P_{d-1}\left(\frac{d\eta-1}{d-1}\right). \tag{3.9}$$

Indeed, the Curie temperature of the square lattice is given by

$$\theta_c^{-1} = P_2(\eta) = \frac{1}{\pi}\ln\frac{8}{1-\eta} \cong \frac{2}{\pi}\ln\frac{4\sqrt{2}}{\kappa_c}. \tag{3.10}$$

The extra factor $3/(2N)$ in Eq. (3.8), relative to this result, is due to the rescaling of the exchange interaction and the number of nearest neighbors in the mean-field transition temperature of Eq. (2.4). Appearance of N under the logarithm in Eq. (3.8) is due to cutting of the integral over q in Eq. (3.3) at $q \sim 1/N$ rather than at the Brillouin-zone boundary: Only in this range of q the film behaves two dimensionally.

For $d < 3$ the integral in Eq. (3.3) for $\kappa_c N \ll 1$ is dominated by $\kappa_c \sim q \ll 1/N$, and the result has the form

$$\theta_c^{-1} \cong P_d(\eta) + \frac{d'}{\Lambda^{d'}}\frac{d\kappa_c^{d-2}}{\kappa_c N}\frac{\pi}{\sin[(3-d)\pi/2]}. \tag{3.11}$$

Note that because of the small factor κ_c^{d-2} in the numerator, both terms of Eq. (3.11) can be comparable with each other. For the square-lattice stripe $d = 2$, the bulk term of Eq. (3.11) can be neglected and the result simplifies to $\theta_c^{-1} = 2/(\kappa_c N)$. This is in absolute accord with Eq. (3.9), since for the chain $P_1(\eta) = 1/\sqrt{1-\eta^2}$. For the continuous-dimension model $d = 2.0$, the the expression for θ_c^{-1} should be multiplied by $\pi/\sqrt{6} \approx 1.283$. It should be noted that the phase transition in chains or stripes can only occur in the limit $D \to \infty$. For any finite D, the long-range order is broken by longitudinal fluctuations which lead to formation of domains.

IV. FREE BOUNDARY CONDITIONS

In a film with fbc, there is an additional disordering due to boundaries that is responsible for the larger suppression of the Curie temperature of a film in comparison to the model with pbc. The greatest difference between the two models arises within the MFA, where for the pbc model T_c is the same as in the bulk and for the hypercubic fbc model one has[7]

$$\theta_c = 1 - \frac{1}{d}\left(1 - \cos\frac{\pi}{N+1}\right). \tag{4.1}$$

This result also can be obtained for the ASM in the limit $\eta \to 0$, where Eq. (2.1) trivializes and the mean-field approximation becomes exact., For the pbc model in this limit, finite-size corrections to T_c disappear as $\exp(-\kappa_c N)$.

For $\eta \neq 0$, the situation for the fbc model becomes complicated, since the gap parameter G_n is nonuniform near the boundaries and cannot be calculated analytically in most cases. This problem becomes, however, nonessential in high dimensions, $d > 4$, as well as in all dimensions for $\kappa_c N \gg 1$. Here the inhomogeneity of G_n is localized to the narrow region near the film boundaries, $n \sim 1$ in the first case[22] and $n \sim 1/\kappa_c \ll N$ in the second case. In the main part of the film, $G_n = G$ is uniform, and its value at the critical point of the film can be obtained from the condition that the *longitudinal* susceptibility diverges, i.e., the determinant of system of equations (2.1) for $\eta = 1$ and $\mathbf{q} = 0$ turns to zero. It is instructive to calculate, instead of the determinant, the whole spin CF from Eq. (2.1) with the free boundary conditions of Eq. (2.5) for the uniform G, ignoring the narrow boundary region where G is nonuniform. The result for the *transverse* CF reads

$$\sigma_{nn}^{\rm fbc}(\mathbf{q}) = \frac{d\theta}{\eta\sqrt{b^2-1}}\frac{[1-\alpha^{2n}][1-\alpha^{2(N+1-n)}]}{1-\alpha^{2(N+1)}}, \tag{4.2}$$

the *longitudinal* CF being given by the same expression with $\eta = 1$. For the bulk CF of Eq. (2.21), as well as for the CF of the pbc model, Eq. (3.1), the divergence corresponds to $b = 1$. This leads, according to Eq. (2.2) with $\eta = 1$ and $\mathbf{q} = 0$, to $G = 1$ at the phase transition point. The pole at $b = 1$ is cancelled, however, in Eq. (4.2), since, according to Eq. (2.20), $b = 1$ entails $\alpha = 1$. The new pole in the fbc correlation function corresponds to $\alpha^{N+1} = -1$, i.e., to

$$\alpha = \exp\frac{i\pi}{N+1}, \qquad b = \frac{1}{2}(\alpha + \alpha^{-1}) = \cos\frac{\pi}{N+1}. \tag{4.3}$$

Now the value of G at the Curie temperature of the film can be found from Eq. (2.2) with $\eta = 1$ and $\mathbf{q} = 0$. The result has the form

$$G^{-1} = 1 - \frac{1}{d}\left(1 - \cos\frac{\pi}{N+1}\right). \tag{4.4}$$

Now θ_c can be found from the constraint relation (2.6) for the *transverse* CF of Eq. (4.2). The integral over the Brillouin zone in Eq. (2.6) simplifies in both cases, $d > 4$ and $\kappa_c N \gg 1$. In high dimensions, the integral is dominated by $q \sim 1$, and at such q the terms with α to high powers beyond the boundary regions can be neglected. The same situation takes place for $\kappa_c N \gg 1$ at all q; in both cases the bulk CF enters under the integral and the the Curie temperature of the film is given by

$$\theta_c^{-1} = GP(\eta G), \tag{4.5}$$

with G defined by Eq. (4.4). In the Ising limit $\eta \to 0$, the mean-field result of Eq. (4.1) is recovered, since $P(0) = 1$. This result is valid for all N, since in this limit $G_n = G$ is uniform throughout the film and all calculations above are exact. If η substantially deviates from zero, this approach works only for large N, where Eq. (4.4) simplifies to

$$G \cong 1 + \frac{1}{2d}\left(\frac{\pi}{N}\right)^2. \tag{4.6}$$

Since the last term in this expression is a small perturbation, Eq. (4.5) can be written in the form[23]

$$\theta_c \cong \frac{1}{P(\eta)}\left[1 - \frac{1}{2d}\left(\frac{\pi}{N}\right)^2 I(\eta)\right], \tag{4.7}$$

where

$$I(\eta) \equiv 1 + \eta P'(\eta)/P(\eta). \tag{4.8}$$

Function $I_d(\eta)$ shows the same qualitative behavior as $P_{d-2}(\eta)$ (see, e.g., Ref. 22). In particular, in the weakly anisotropic case $\kappa_c \ll 1$ [see Eq. (2.13)], one has

$$I(\eta) \cong \begin{cases} \tilde{C}_d/\kappa_c^{4-d}, & 1 \le d \le 4 \\ I(1) - \tilde{C}_d\kappa_c^{d-4}, & 4 < d < 6. \end{cases} \tag{4.9}$$

For $d > 4$, $I(\eta)$ remains finite in the isotropic limit, $\eta \to 1$. In this dimensionality range formula (4.7) works for all anisotropies, as was argues above. In the marginal case $d = 4$, $I(\eta)$ diverges logarithmically for $\eta \to 1$. For the hypercubic lattice, Eq. (4.7) takes the form

$$\theta_c^{-1} \cong P_4(1) + \frac{1}{N^2}\ln\frac{c}{\kappa_c}, \qquad c \sim 1. \tag{4.10}$$

If anisotropy becomes so small that $\kappa_c N \lesssim 1$, then the integral over the Brillouin zone in the constraint relation is cut at the lower limit $q \sim 1/N$ instead of $q \sim \kappa_c$. This leads to the result

$$\theta_c^{-1} \cong P_4(1) + \frac{\ln N}{N^2} + \frac{C}{N^2}, \tag{4.11}$$

where $C \sim 1$ cannot be calculated analytically. For the continuous-dimension lattice $d = 4.0$, one should, according to Eq. (3.5), insert the factor $3\pi/(5\sqrt{10}) \approx 1.873$ in front of the logarithms in the above equations.

For $d < 4$, $I(\eta)$ and thus the finite-size correction to T_c given by Eq. (4.7) diverges in the isotropic limit, $\eta \to 1$.

In the dimensionality range $3 < d < 4$, however, the latter does not imply that T_c goes to zero, since the film is a system of dimension $d' = d - 1$ and it can still order without anisotropy for $d' > 2$. In fact, the situation here is determined by small wave vectors, $q \lesssim 1/N \ll 1$, in contrast to $q \sim 1$ for $d > 4$. In this wave-vector range d'-dimensionality of the film manifests itself by the appearance of an additional power of q in the denominator of the spin CF $\sigma_{nn}(\mathbf{q})$. Dimensional arguments show that this should be the combination $N\sqrt{\kappa^2 + q^2} \lesssim 1$. Thus the finite-size correction to T_c has the form

$$\theta_c^{-1} - P_d(\eta) \sim \frac{1}{N} \int_0^{1/N} \frac{dq q^{d-2}}{\kappa^2 + q^2}, \tag{4.12}$$

which leads to the same dependence $\Delta T_c \equiv T_c(\infty) - T_c(N) \propto 1/N^{d-2}$ as for the model with pbc, Eq. (3.4). Analytical calculation of the numerical factor in this dependence seems to be very difficult or impossible, because it requires knowing of the self-consistently determined variation of G_n in the film. This numerical factor should be larger that for the model with pbc because of the additional disordering at the film boundaries. One can see that for $d < 4$ this contribution to the shift of T_c is larger than the contribution $\Delta T_c \propto 1/N^2$ from the region $q \sim 1$, which is described by Eq. (4.7). At large distances $N \gtrsim 1/\kappa_c$, the wave-vector range in which the film behaves d'-dimensionally disappears, as can be seen from Eq. (4.12). Here a crossover to the regime of Eq. (4.7) occurs.

For $d \leq 3$, the intergal in Eq. (4.12) diverges at the lower limit in the isotropic case. In this range, the dimensionality of the film is $d' \leq 2$ and it cannot order without anisotropy. For very small anisotropies, T_c of the film is very low, and at such temperatures the chains of spins going from one boundary to the other are strongly correlated and behave as single composite spins, as was explained in the Introduction. Here the situation simplifies, and the type of boundary conditions no longer plays a role in the determination of T_c that is given by Eq. (3.9). In the marginal case $d = 3$, the corresponding formula has only logarithmic accuracy,[23] and the more accurate result for the simple cubic lattice has the form

$$\theta_c^{-1} \cong P_3(\eta) + \frac{3}{\pi N} \ln \frac{1}{\kappa_c N} + \frac{C}{N}, \tag{4.13}$$

where $C \sim 1$ should be calculated numerically [cf. Eq. (4.13)] . It is interesting to note that the variation of G_n throughout the film can be easily found in the limit under consideration. It adjusts in a way that is compatible with the full correlation of the film's layers, i.e., with $\sigma_{nn'}$ being the same for all n and n' at small q. The latter requires that all α_n and α'_n in Eq. (2.19) are close to 1. Then from Eq. (2.18) one finds that $b_n \cong 1$ inside the film. On the contrary, in the boundary layers one obtains $b_1 = b_N \cong \frac{1}{2}$. The resulting variation of G_n in the film can now be determined from Eq. (2.2) and has the form

$$G_n \cong \begin{cases} \dfrac{2d}{2d-1}, & n = 1, N \\ 1, & n \neq 1, N. \end{cases} \tag{4.14}$$

To conclude this section, let us consider the bilayer, $N = 2$. For the bilayer, Curie temperature can be calculated analytically with the help of the diagonalization formalism described at the end of Sec. II. At T_c one has $G_1 = G_2 = 2d/(2d-1)$, and the Curie temperature ifself is given by

$$\theta_c^{-1} = \sum_{\pm} \frac{d}{2d - 1 \pm \eta} P_{d-1}\left(\frac{2(d-1)\eta}{2d-1\pm\eta}\right), \tag{4.15}$$

where $\sum_{\pm}$ sums terms with both signs. In dimensions $d \leq 3$, the term with the sign minus diverges in the isotropic limit, $\eta \to 1$, whereas the term with the sign plus remains finite. In this case the result is compatible with the general-N formula (3.9).

For films consisting of larger number of layers, the diagonalization formalism becomes cumbersome. For $N = 3$, in particular, the cubic characteristic equation for the problem simplifies, and one can write down analytical expressions for the correlation functions in terms of $G_1 = G_3$ and G_2. The latter and the Curie temperature, however, are defined by a system of transcedental equations that cannot be solved analytically.

V. NUMERICAL RESULTS

The system of equations describing the anisotropic spherical model was solved numerically in the following way. For a given variation of G_n, the transverse layer-layer autocorrelation functions σ_{nn} were found with the help of Eqs. (2.17) and (2.18). The results were substituted into the constraint relations (2.6) to obtain, after the integration over $\mathbf{q}$, the system of nonlinear equations for the set of G_n. The latter was solved by the Newton method. In fact, all equations were rewritten in terms of deviations from the bulk values (see Ref. 22), which helps to improve the accuracy. This calculation yield the variation of G_n throughout the film for any temperature $T \geq T_c$. To find the value of T_c, the nonlinear equation in temperature, $\mathcal{D}(T) = 0$, was solved, where $\mathcal{D}(T)$ is the determinant of system of linear equations (2.1) for $\eta = 1$ and $\mathbf{q} = 0$. In this system of equations, the values of b_n are given by Eq. (2.2), where G_n are functions of temperature found on the previous step of the numerical routine.

It is convenient to plot, instead of G_n, its deviation from the bulk value $G_{1n} \equiv G_n - G$ which at and below the bulk criticality (i.e., for $G = 1$) is equal to the nonuniform part of the reduced energy density $\tilde{U}_{1n}$.[22] The variations of G_{1n} in the isotropic films at bulk and film criticalities in four and five dimensions for the continuous-dimension model are shown in Fig. 1. The results for the hypercubic lattice differ from the latter by nonuniversal factors of order unity and are not shown. One can see that for

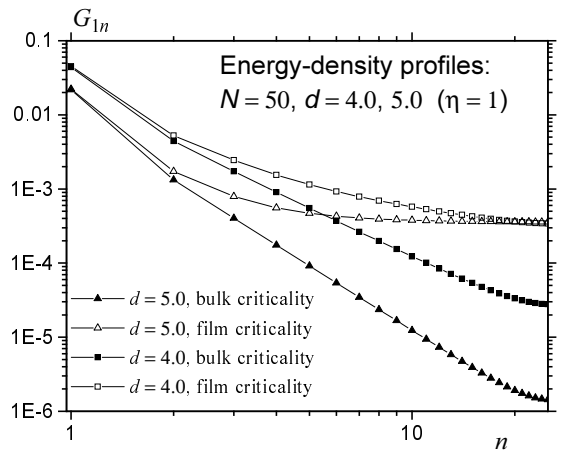

FIG. 1. Energy-density profiles at bulk and film criticalites for the isotropic $D = \infty$ model in four and five dimensions.

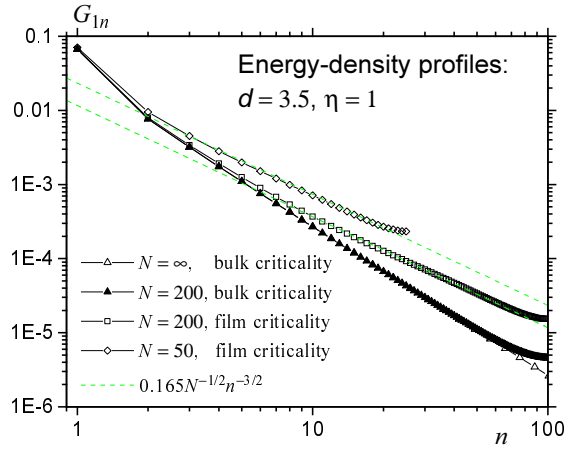

FIG. 2. Energy-density profiles at bulk and film criticalites for the isotropic $D = \infty$ model in dimension $d = 3.5$.

$d = 5$ at the film criticality the value of G_{1n} is close to $(\pi/N)^2/(2d) \approx 4 \times 10^{-4}$ in the main part on the film, in accordance with Eq. (4.4). The bulk-criticality profiles of G_{1n} that are plotted for comparison, show a very different behavior. They follow the appropriate semi-infinite profiles $G_{1n} \sim 1/n^{d-2}$ (Ref. 22) until approximately $n \sim N/4$. Crossing of the latter with the plato level at some $n^* \sim N^{2/(d-2)}$ determines the boundary region $n \lesssim n^*$ where the semi-infinite G_{1n} profile is realized. For $d > 4$, the value of n^* increases slowlier that N; thus for thick films the plato of G_{1n} dominates the film's Curie temperature, as was explained in Sec. IV In the marginal case $d = 4$, the plato of G_{1n} is much less pronounced. In fact, it arises only for $\ln N \gg 1$.

For $d < 4$, the problem becomes more complicated, and no analytical solution for the variation of G_{1n} could be obtained. Numerical results for $d = 3.5$ that are shown in Fig. 2 are also different for film and bulk criticalities. At the film criticality, the power-law dependence $G_{1n} \approx 0.165N^{-1/2}n^{-3/2}$ is seen, instead of a plato. For comparison, the dependence of G_{1n} in the

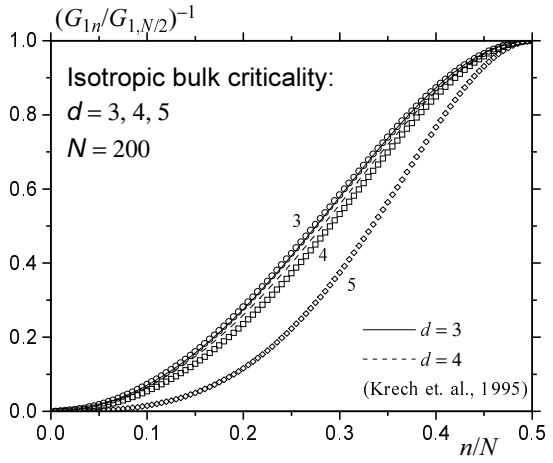

FIG. 3. Reciprocal of normalized energy-density profiles at bulk criticalites for the isotropic $D = \infty$ model in dimensions $d = 3, 4$ and 5.

semi-infinite geometry, which is given by Eq. (2.14), has the form $G_{1n} \approx 0.0268n^{-2}$ for $d = 3.5$. It is clear that for very thick films both criticalities are very close to each other, and, at the film criticality, the semi-infinite solution should be realized in some region not too far from the boundary. The crossover from this solution to the numerically found $n^{-3/2}$ law can be located by equating the expressions above. The result is that for $d = 3.5$ at the film criticality, the semi-infinite solution is realized in the region $1 \ll n \lesssim n^*$ with $n^* \approx 0.0264N$, whereas the $n^{-3/2}$ law holds for $n^* \lesssim n$ but not too close to the center of the film (see Fig. 2). What is the nature of the numerical parameter 0.0264? Is it small enough to allow an analytical derivation of the $n^{-3/2}$ law? These questions have not been addressed in this article.

For $d \leq 3$, the film's Curie temperature and the energy-density profile at the film criticality depend on anisotropy in an essential way. This makes the corresponding figures less interesting; in particular, for $\kappa_c N \gg 1$ there is a plato of G_{1n} at the distances from the boundaries $n \gtrsim 1/\kappa_c$. By contrast, energy-density profiles at the bulk criticality can be studied for $d > 2$ for isotropic models. This problem for the semi-infinite and film geometries can be addressed with field-theoretical methods for systems with an arbitrary number of spin components D (see, e.g., Refs. 27 and 28). In Refs. 29 and 30, the energy-density profiles in critical films with various boundary conditions have been calculated with the help of the ϵ expansion. For the free boundary conditions considered here, the exponentiated energy-density profile g is given by Eq. (5.7) of Ref. 30. In the limit $D \to \infty$ one can use $\nu = 1/2$ and $\nu = 1$ in four and three dimensions, respectively, and for $d = 4$ and $d = 3$ the result of Ref. 30 simplifies to

$$g_4(x) = \frac{\pi^2}{\sin^2 \pi x} - \frac{\pi^2}{3}$$

$$g_3(x) = -[\psi(x) + \psi(1-x) + 2\gamma]\frac{\pi}{\sin \pi x} - \frac{\pi^2}{6}, \qquad (5.1)$$

where z is the distance from the left boundary, L is the film thickness, $x \equiv z/L = n/N$, $\psi(x) \equiv \Gamma'(x)/\Gamma(x)$, and $\gamma = 0.57721566\ldots$ The quantity $g(x)$, by definition, may differ from G_{1n} only by a numerical factor which is dependent on N. Thus the reduced quantity $\tilde{g}(x) \equiv g(x)/g(0.5)$ can be compared with the G_{1n} profiles numerically calculated for the isotropic $D = \infty$ model, which are shown in the scaled form in Fig. 3. One can see that for $d = 3$ the agreement is reasonably good, keeping in mind that $g_3(x)$ of Eq. (5.1) has been obtained in the first order in $\epsilon = 4 - d$. The curve $1/\tilde{g}_4(x)$, however, goes in the middle between the curves representing the numerical results for $d = 4$ and $d = 3$. The origin of this discrepancy is that $g_4(x)$ of Eq. (5.1) does not comprise logarithmic terms which appear in four dimensions. In particular, for the semi-infinite problem in four dimensions one has[22] $G_{1n} = [16n^2 \ln(an)]^{-1}$ with $a \sim 1$ for $n \gg 1$. By contrast, both g_4 and g_3 simplify to $g(x) = 1/x^2$ for $x \ll 1$, which corresponds to the the semi-infinite case. For $d > 4$, the variation of G_{1n} can be found analytically, at least at or above the bulk criticality, by the integration of the free proparator, as was done for the semi-infinite problem in Sec. IIIC of Ref. 22. This routine coincides with that used in Ref. 30 in the film geometry up to numerical factors; thus the results of both approaches, in the scaled form, are identical in high dimensions. For $d = 4$, however, logarithmic term appears in the method of Ref. 22, in contrast to that of Ref. 30.

Another possible normalization of the energy-density profiles is that with respect to the solution of the semi-infinite problem G^{∞}_{1n}. The function $\bar{g}(n/N) \equiv G_{1n}/G^{\infty}_{1,N/2}$ contains more information than $\tilde{g} \equiv G_{1n}/G_{1,N/2}$ used above. In particular, the value of $\bar{g}$ in the middle of the film can be used to compare the accuracy of different approaches. So, for $d = 3$ the numerical calculation yields $\bar{g}_3(0.5) \approx 1.822$. For $d = 4$, the value of $\bar{g}(0.5)$ slightly increases with N because of the logarithmic corrections to scaling: One obtains $\bar{g}_4(0.5) \approx 1.772$ for $N = 100$ and $\bar{g}_4(0.5) \approx 1.795$ for $N = 200$. On the other hand, the results of Ref. 30 are scaled as $\bar{g}(x) = g(x)/4$; thus from Eq. (5.1) one obtains $\bar{g}_3(0.5) \approx 1.766$ and $\bar{g}_4(0.5) \approx 1.645$. One can see that the discrepancy between the exact solution for the $D = \infty$ model presented here and the field-theoretical results of Ref. 30 is comparable to the difference between the results for $d = 3$ and $d = 4$.

It is interesting to note that the numerical solution for $d = 3$ can be represented with a pretty good accuracy by the empirical formula

$$\bar{g}(n/N) \equiv \frac{G_{1n}}{G^{\infty}_{1,N/2}} = \frac{(\pi/2)^{4/3}}{\sin^{4/3}[(\pi/2)(2x)^{3/2}]}. \qquad (5.2)$$

In Fig. 3, the corresponding curve would go exactly over the circles for $d = 3$, so it is not shown. The value $\bar{g}(0.5) = (\pi/2)^{4/3} \approx 1.826$ is very close to the numerically calculated value 1.822 cited above.

Numerical results for the relative shift of T_c in isotropic films with free boundary conditions in high dimensions

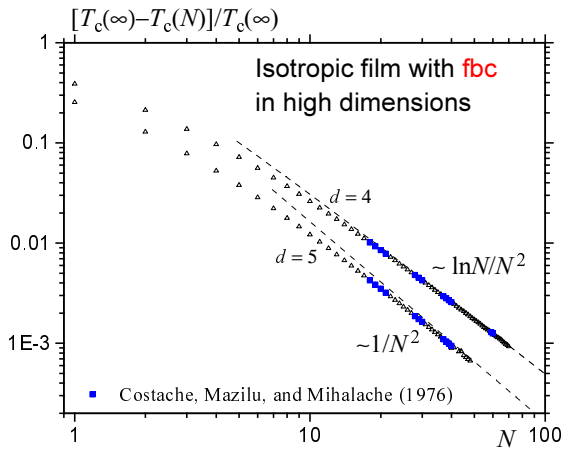

FIG. 4. Curie-temperature shift in films with fbc for the isotropic $D = \infty$ model in four and five dimensions (continuous-dimension model).

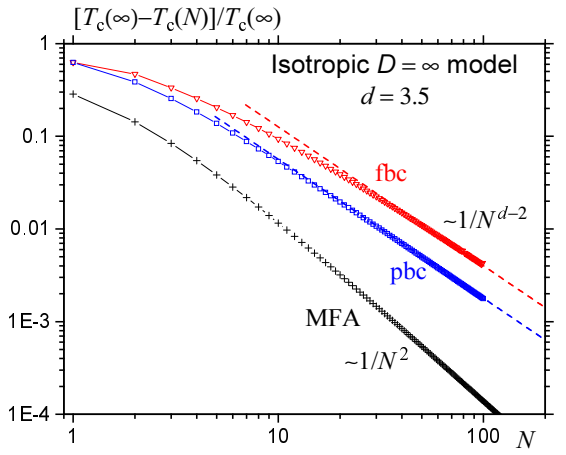

FIG. 5. Curie-temperature shift in films with fbc for the isotropic $D = \infty$ model in dimension $d = 3.5$.

are shown in Fig. 4. For $d = 5$, the data approach at large N the asymptotic formula (4.7) with $I_5(1) \approx 1.66$. For $d = 4$, the results for thick films follow Eq. (4.11) with $C \approx 1.5$. Both of these asymptotes are shown by dashed lines in Fig. 4. For both hypercubic lattices, the data are in accord with those of Ref. 16, where a spherical model with separate spin constraints in each of the layers was used. This modified spherical model is thus better than the standard one using the global spin constraint. However, it cannot be generalized for the anisotropic case and applied to films in three dimensions.

To illustrate the situation in the range $3 < d < 4$ where the isotropic $D = \infty$ model shows nontrivial power law for the T_c shift in films, the data for $d = 3.5$ are shown in Fig. 5. One can see that both models with pbc and fbc show the same shift exponent $\lambda = d - 2$. For the model with pbc, the amplitude A in Eq. (1.1) calculated from Eq. (3.4) is $A \approx 1.788$. For the fbc model, one obtains $A \approx 4$ from the fit to the numerical results. This value is substantially larger than for the model with pbc because

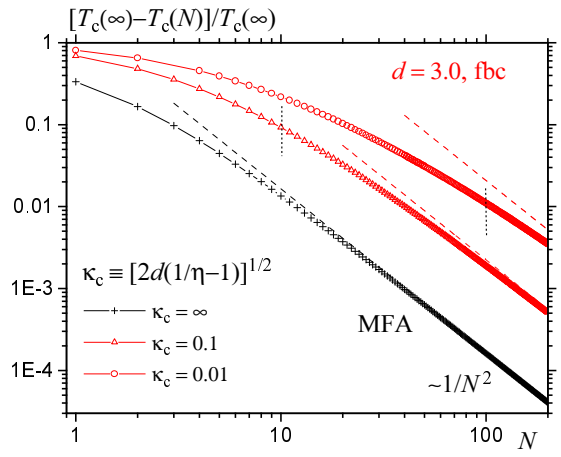

FIG. 6. Curie-temperature shift in films with fbc for the ASM in three dimensions (continuous-dimension model). The crossover values of N corresponding to $\kappa_c N = 1$ are shown by short vertical lines.

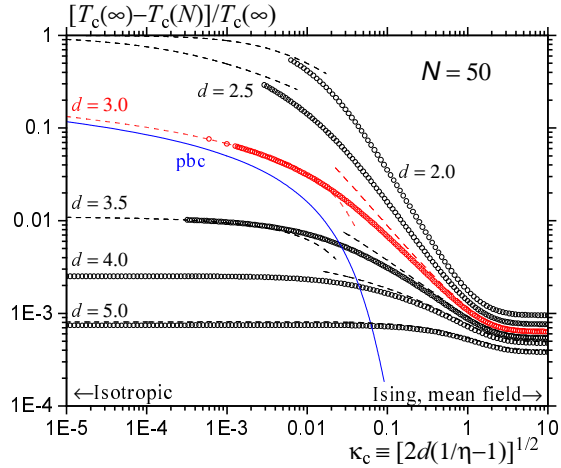

FIG. 7. Curie-temperature shift in films with fbc for the ASM in different dimensions vs anisotropy (continuous-dimension model). High- and low-anisotropy asymptotes are shown by dashed lines.

of the boundary effects that affect the whole sample (see Fig. 2). Also due to the boundary effects, the data approach the power-law asymptote much slowlier than for the pbc model.

Numerical results for the T_c shift in films with fbc in there dimensions for different values of the anisotropy are shown in Fig. 6. The data follow Eq. (4.13) at $\kappa_c N \lesssim 1$ and Eq. (4.7) for larger thicknesses, $\kappa_c N \gtrsim 1$. In the latter case, the shift exponent in Eq. (1.1) is $\lambda = 2$, as in the mean-field case, but the amplitude A can be very large for small anisotropy.

Finally, the dependences of the T_c shift in films of $N = 50$ layers in different dimensions are shown as function of the anisotropy in Fig. 7. For $d = 5$, the data are well described by the formula (4.7) anisotropy range. For $d = 4$, this formula fails at small anisotripies because of the logarithmic divergence of $I_4(\eta)$ at $\eta = 1$ and it should be replaced by Eq. (4.11) in the isotropic limit. For $d = 3.5$, the Newton algorithm for finding T_c fails at small anisotropies because the inverse longitudinal susceptibility of a film or the determinant of the linear system of equations (2.1) approach zero very flat: $\chi_z^{-1}(T) \propto \mathcal{D}(T) \propto (T - T_c)^{2/(d-3)}$ in the isotropic case. Knowing this dependence, one can go over to the equation for the nonlinearly scaled quantity, e.g., $\mathcal{D}^{(d-3)/2}$, that behaves linearly near T_c. In such a way, in fact, the data in Fig. 5 have been obtained. This yields $T_c(N)/T_c(\infty) \approx 0.989$ for $d = 3.5$ in the isotropic limit. The functional form of the dependence of T_c on anisotropy near the isotropic limit can be found from the observation that the film behaves as a d'-dimensional system in the wave-vector range $qN \lesssim 1$. One can write [cf. Eq. (2.10)]

$$\frac{T_c(N)}{T_c(\infty)} \cong \left.\frac{T_c(N)}{T_c(\infty)}\right|_{\kappa_c=0} \times \left(1 + \frac{c_d \kappa_c^{d-3}}{N}\right), \qquad (5.3)$$

where c_d should be determined numerically. Fit to the data for $d = 3.5$ yields $c_{3.5} \approx 2.40$. With this choice, asymptote (5.3) overlaps with the numerical results in Fig. 7 in a sufficiently wide range of κ_c.

In three dimensions, $T_c(N)$ goes to zero logarithmically in the isotropic limit according to Eq. (4.13). The fit to the numerical data for the continuous-dimension lattice [$3/\pi$ in front of the logarithm in Eq. (4.13) is replaced by $3/2$] yields $C = 1.77$. Again, this asymptote well fits the numerical data in a wide range of anisotropies.

For $d < 3$, the Curie temperature of the film goes to zero as $T_c \propto N\kappa_c^{3-d}$ in the isotropic limit, in accordance with Eq. (3.11). The corresponding asymptotes for $d = 2.5$ and $d = 2.0$ are shown by dashed lines in Fig. 7. Unfortunately, numerical calculations could not been performed for such small anisotropies because of the instability of the numerical algorithm.

VI. DISCUSSION

In this paper a profound influence of the anisotropy on ordering in ferromagnetic films has been investigated. The main result is that in three dimensions, the behavior of the film of arbitrary number of monolayers N can be dominated, for sufficiently small anisotropy, by two-dimensional fluctuations which strongly suppress the ordering temperature. *Films described by the isotropic Heisenberg model cannot order in three dimensions.* Most of results above have been obtained for the exactly solvable infinite-component spin-vector model, but more realistic models as the Heisenberg model should share the same qualitative behavior. In particular, the small-anisotropy formula for T_c, Eq. (1.2), should be valid for all models in dimensions less than three. In this dimensionality range, the shift amplitude A in Eq. (1.1) should diverge in the isotropic limit for all systems.

The theoretical tool used here, the anisotropic spherical model, allows to separate the major effects of Goldstone or would be Goldstone modes in systems of reduced

dimensionality from usually less significant but complicative effects of critical fluctuation coupling. The ASM has a lot of advantages in comparison to the mean-field approximation or to the standard spherical model, and it should be tried for classsical spin systems the next after the MFA. Some more subtle effects, as the Berezinsky-Kosterlitz-Thouless phase transition, are, however, not reproducible within the ASM.

A peculiar feature of the ASM is that only fluctuations transverse with respect to the easy axis give contribution to the equations describing static properties of the system. Thus these equations contain the transverse correlation length $\xi_{c\perp} \equiv 1/\kappa$ as the length scale. In particular, crossover between different regimes for the Curie temperature of the film, $T_c(N)$, occurs at $\kappa_c N \sim 1$, where κ_c is given by Eq. (2.13). The longitudinal correlation function and longitudinal correlation length are the "slave" quantities that are decoupled from the system of equations for the ferromagnet and can be determined after the solution of the latter. By contrast, in the conventional theory of phase transitions the diverging longitudinal correlation length is used as the length scale. It would be interesting to see how does it appear in the theory of ordering in films, if one goes beyond the $D = \infty$ model, i.e., takes into account the $1/D$ corrections.

A more urgent task, however, is to solve the system of equations describing the anisotropic spherical model below T_c, both in the semi-infinite and film geometries.

To conclude, it should be noted that equations resembling those describing the ASM can be obtained for quantum systems in spirit of the random-phase approximation by decoupling of the high-order Green functions. Examples of such works in the film geometry are Refs. 25 and 31.

* Permanent address: I. Institut für Theoretische Physik, Universität Hamburg, Jungius Strasse 9, D-20355 Hamburg, Germany.
Electronic addresses: garanin@mpipks-dresden.mpg.de
garanin@physnet.uni-hamburg.de
http://www.mpipks-dresden.mpg.de/∼garanin/

[1] C. A. Neugebauer, Phys. Rev. **116**, 1441 (1962).
[2] U. Gradmann, Appl. Phys. **3**, 161 (1974).
[3] W. Dürr, M. Taborelli, O. Paul, R. Germer, W. Gudat, D. Pescia, and M. Landolt, Phys. Rev. Lett. **62**, 206 (1989).
[4] Yi Li and K. Baberschke, Phys. Rev. Lett. **68**, 1208 (1992).
[5] P. Schilbe, S, Siebentritt, and K.-H. Rieder, Phys. Lett. A **216**, 20 (1996).
[6] K. Baberschke, Appl. Phys. A **62**, 417 (1997).
[7] T. Wolfram, R. E. Dewames, W. F. Hall, and P. W. Palmberg, Surf. Sci. **28**, 45 (1971).
[8] G. A. T. Allan, Phys. Rev. B **1**, 352 (1970).
[9] M. E. Fisher, in *Critical Phenomena*, edited by M. S. Green (Academic Press, New York, 1971), Vol. 2.
[10] M. E. Fisher and M. N. Barber, Phys. Rev. Lett. **28**, 1516 (1972).
[11] M. N. Barber, in *Phase Transitions and Critical Phenomena*, edited by C. Domb and J. L. Lebowitz (Academic Press, New York, 1983), Vol. 8.
[12] H. E. Stanley, Phys. Rev. **176**, 718 (1968).
[13] T. N. Berlin and M. Kac, Phys. Rev. **86**, 821 (1952).
[14] M. N. Barber and M. E. Fisher, Ann. Phys. (N.Y.) **77**, 1 (1973).
[15] H. J. F. Knops, J. Math. Phys. **14**, 1918 (1973).
[16] G. Costache, D. Mazilu, and D. Mihalache, J. Phys. C **9**, L501 (1976).
[17] D. A. Garanin and V. S. Lutovinov, Solid State Commun. **50**, 219 (1984).
[18] D. A. Garanin, Z. Phys. B **102**, 283 (1997).
[19] D. A. Garanin and B. Canals, Phys. Rev. B (submitted, cond-mat/9805362).
[20] D. A. Garanin, J. Phys. A **29**, 2349 (1996).
[21] J. Kötzler, D. A. Garanin, M. Hartl, and L. Jahn, Phys. Rev. Lett. **71**, 177 (1993).
[22] D. A. Garanin, Phys. Rev. E (in press, cond-mat/9803230).
[23] D. A. Garanin, J. Phys. A **29**, L257 (1996).
[24] A. J. Bray and M. A. Moore, Phys. Rev. Lett. **38**, 735 (1977); J. Phys. A **10**, 1927 (1977).
[25] D. Mihalache, Phys. Lett. A **59**, 295 (1976).
[26] D. O'Connor, C. R. Stephens, and A. J. Bray, J. Stat. Phys. **87**, 273 (1997).
[27] H. W. Diehl, in *Phase Transitions and Critical Phenomena*, edited by C. Domb and J. L. Lebowitz (Academic Press, London, 1986), Vol. 10, pp. 75–267.
[28] H. W. Diehl, Int. J. Mod. Phys. B **11**, 3503 (1997).
[29] E. Eisenriegler, M. Krech, and S. Dietrich, Phys. Rev. Lett. **70**, 619 (1993).
[30] M. Krech, E. Eisenriegler, and S. Dietrich, Phys. Rev. E **52**, 1345 (1995).
[31] V. Yu. Irkhin, A. A. Katanin, and M. I. Katsnelson, J. Magn. Magn. Mater. **164**, 66 (1996).